

Formation of a bilayer ordered surface alloy Mn/Ag(001)

Wondong Kim, Wookje Kim, and S.-J. Oh

Department of Physics, Seoul National University, Seoul 151-742, Republic of Korea

J. Seo

Division of General Education, Cho-Dang University, Muan 524-800, Republic of Korea

J.-S. Kim

Department of Physics, Sook-Myung Women's University, Seoul 140-742, Republic of Korea

H.-G. Min

Department of Physics, Hong-Ik University, Seoul 121-791, Republic of Korea

S.-C. Hong

*Department of Physics, University of Ulsan, Ulsan 680-749, Republic of Korea
and Department of Physics and Astronomy, Northwestern University, Evanston, Illinois 60208-3112*

(Received 26 August 1997)

Low-energy electron diffraction I/V analyses reveal that Mn thin films deposited on Ag(001) at room temperature form substitutional, ordered, bilayer $\text{Mn}_{50}\text{Ag}_{50}$ surface alloys. The Mn atoms in this structure have local magnetic moments of considerable value, as judged from the Mn $3s$ core level spectra; these local magnetic moments of Mn are effective in the formation of the ordered surface alloy. *Ab initio* total energy calculations have been done and the results confirmed the experimental observations.
[S0163-1829(98)03611-X]

Mn thin films on various noble metal systems have attracted a great deal of attention because of the close relation between their magnetic properties and geometrical structure.^{1,2} In search of the correlation between structure and magnetism, the Mn/Ag(001) system has been a particular focus for some time. Newstead *et al.* observed a $c(2 \times 2)$ low-energy electron diffraction (LEED) pattern for Mn/Ag(001) in the thickness range of 0.5–1.5 monolayers (ML) (Ref. 3) and suggested that it was due to the Mn overlayer structure. They also observed a reduced exchange splitting in the Mn $3s$ core level spectrum for 1-ML-thick Mn films, and concluded that this indicates a reduction of the local magnetic moment of Mn due to hybridization with Ag. After this study, some experiments were performed for Mn thin films a few monolayers thick on Ag(001), but a clear conclusion was not drawn for the monolayer regime.^{4,5} Recently, the results of inverse photoemission spectroscopy (IPES) experiments showed the possibility of a well-ordered surface structure for one monolayer thickness.⁶ More recent x-ray photoelectron diffraction (XPD) experiments⁷ indicate that submonolayer Mn atoms evaporated on Ag(001) form a surface alloy by intermixing with Ag atoms and that the thickness of intermixing depends on the growth temperature. They also observed a $c(2 \times 2)$ LEED pattern, but did not discuss its origin in connection with their XPD result.

In this paper, we present results of LEED I/V analyses mainly on the 1 ML Mn/Ag(001) system. Between 0.5 and 1.5 ML Mn, a bright $c(2 \times 2)$ pattern is found, as in previous studies, and at 1 ML, the LEED pattern is at its best with sharp and intense half-order spots and low background. According to our analysis of LEED I/V curves on this 1 ML

Mn/Ag(001) system, this $c(2 \times 2)$ pattern originates from a bilayer ordered surface alloy formed of evaporated Mn. This “bilayer” growth mode has not been observed before for any other surface alloy system, although single-layer ordered alloys have been reported.⁸ To obtain information about the local magnetic moment of Mn, we also carried out x-ray photoemission experiments. A substantial local magnetic moment can be deduced from the observed $3s$ exchange splitting (~ 4.0 eV) of Mn atoms in the bilayer alloy, unlike the results of previous work.³ To confirm our observation, *ab initio* total energy calculations were performed and found to be in good agreement with the experimental results.

The Ag(001) single-crystal substrate used in this experiment was a tophat-shaped disk 8 mm in diameter and 1 mm thick. After several repeated cycles of Ar^+ ion bombardment and annealing at 800 K, the crystal surface showed a sharp $p(1 \times 1)$ LEED pattern and no contamination was detected by Auger electron spectroscopy using a cylindrical mirror analyzer. Mn was evaporated onto the clean Ag(001) surface from a source consisting of a Mn chip wound around W filaments; the typical evaporation rate was ~ 1 ML per 5 min. The Mn coverage was determined from the intensity ratio of Mn (539 eV) and Ag (359 eV) Auger peaks. The base pressure was 5×10^{-11} Torr and was maintained below 2×10^{-10} Torr during Mn evaporation. X-ray photoemission spectroscopy (XPS) experiments were carried out in another UHV chamber, where a LEED analyzer, an x-ray source, and a concentric hemispherical electron energy analyzer were installed. The base pressure of this chamber was 1×10^{-10} Torr and maintained under 1×10^{-9} Torr during evaporation. The overall spectrometer resolution was estimated as around

TABLE I. R_p factor for various model structures.

$\text{Mn}_{50}\text{Ag}_{50}/\text{Ag}(001)$	0.4698
$2\text{Mn}_{50}\text{Ag}_{50}/\text{Ag}(001)$	0.2667
$3\text{Mn}_{50}\text{Ag}_{50}/\text{Ag}(001)$	0.3361
$\text{Mn}_{50}\text{Ag}_{50}/\text{Mn}_{100}/\text{Ag}(001)$	0.3187
$\text{Ag}_{100}/\text{Mn}_{50}\text{Ag}_{50}/\text{Ag}(001)$	0.3662
$\text{Mn}_{100}/\text{Mn}_{50}\text{Ag}_{50}/\text{Ag}(001)$	0.4010
$\text{Ag}_{100}/\text{Mn}_{50}\text{Ag}_{50}/\text{Mn}_{50}/\text{Ag}(001)$	0.3223
<hr/>	
$\text{Mn}_{50}/\text{Ag}(001)$	0.5847
$\text{Mn}_{50}/\text{Mn}_{50}\text{Ag}_{50}/\text{Ag}(001)$	0.3582
$\text{Mn}_{50}/\text{Ag}_{100}/\text{Mn}_{50}\text{Ag}_{50}/\text{Ag}(001)$	0.6808
$\text{Ag}_{50}/\text{Mn}_{50}\text{Ag}_{50}/\text{Ag}(001)$	0.4011
$\text{Ag}_{50}/2\text{Mn}_{50}\text{Ag}_{50}/\text{Ag}(001)$	0.4180
$\text{Ag}_{50}/\text{Mn}_{100}/\text{Ag}(001)$	0.4583
$\text{Mn}_{50}/2\text{Mn}_{50}\text{Ag}_{50}/\text{Ag}(001)$	0.4817

1.2 eV. Thickness calibration in the XPS experiments was done by the intensity ratio between Mn $2p$ and Ag $3d$ core level peaks.

For 1 ML Mn deposited on Ag(001) at room temperature, LEED I - V curves were obtained for five symmetrically inequivalent beams including a $(1/2, 1/2)$ beam between 40 and 300 eV by a fully automated video LEED system.⁹ A LEED I/V analysis was done by employing the TENSOR LEED program.¹⁰ Scattering phase shifts¹¹ up to angular momentum quantum number l equal to 6 were used, and thermal vibration effects were taken into account by a Debye-Waller factor with a Debye temperature of 440 K for Mn and 225 K for Ag. An evaluation of the best fit between theory and experiment and the error bar in the structure determination was done with the Pendry R factor (R_p) and its variance.¹²

Two categories of model structures which could generate half-order LEED spots were tested: the first with Mn overlayers and the other with ordered Mn surface alloys. Since the thickness calibration by Auger intensity ratio is dependent on the growth mode, the Auger intensity ratios for our nominal 1 ML Mn film in reference to the bilayer alloy may be obtained for other growth models. Hence we tried to fit the experimental I/V curves for various growth models with $c(2 \times 2)$ symmetry and which give similar Auger intensity ratios, as shown in Table I. The minimum value of the R_p factor, 0.2667, was obtained for the case of a bilayer surface alloy. For other model structures, distinctively higher values were produced.

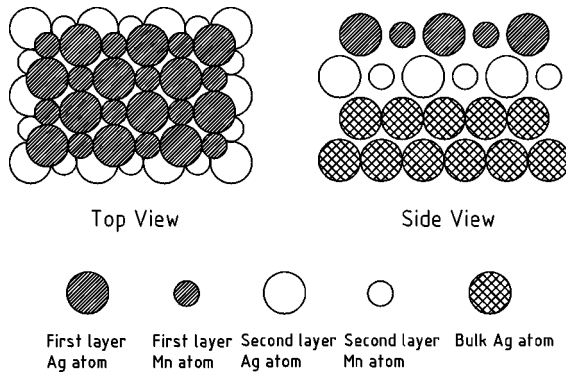
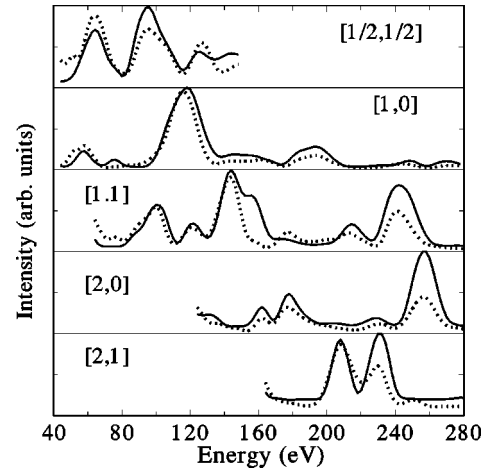
FIG. 1. Schematic diagram of the bilayer $c(2 \times 2)$ surface alloy.

FIG. 2. Experimental (solid line) spectra for the 1 ML Mn/Ag(001) structure and the best fit theoretical spectra (dashed line) by the bilayer surface alloy model structure.

A schematic picture of the bilayer structure is presented in Fig. 1. The calculated spectra for this structure are presented along with experimental I - V curves in Fig. 2. The peak positions and intensity ratio are well reproduced, as expected from the low value of the R factor. The interlayer spacings between the first three layers (d_{12}, d_{23}) and the corrugation in the two alloy layers ($\Delta z = z_{\text{Mn}} - z_{\text{Ag}}$) obtained from the optimized structure are listed in Table II. A small corrugation of 1.7% is found only in the first alloy layer. The interlayer spacing between the first two layers is contracted by a small amount, 0.35%, referred to the interlayer spacing of bulk Ag; otherwise, the contraction between the second and third layers is very large, but this may only reflect the insensitivity of LEED to the atomic structure of the Ag atoms in the third layer as noticed from the large error bar of $\pm 4.9\%$.

To confirm the results of the above LEED analysis, we performed total energy and atomic force calculations for some systems related to our current study, employing the full-potential linearized augmented plane wave (FLAPW) method.¹³ The systems considered were a monolayer of Mn as overlayer [$\text{Mn}_{100}/\text{Ag}(001)$], one monolayer [$\text{Mn}_{50}\text{Ag}_{50}/\text{Ag}(001)$], and two monolayers [$2\text{Mn}_{50}\text{Ag}_{50}/\text{Ag}(001)$] of $c(2 \times 2)$ MnAg ordered alloy layers on Ag(001) and a monolayer subsurface Mn system [$\text{Ag}_{100}/\text{Mn}_{100}/\text{Ag}(001)$]. These systems were simulated as a single slab consisting of 7 ML. On each side of the slab, a Mn overlayer or MnAg alloy layers were placed according to each growth model; the inner layers were Ag. The total en-

TABLE II. Optimized atomic positions of the bilayer surface alloy system by the tensor LEED algorithm and total energy calculation. d_b is interlayer spacing of bulk Ag. (+, extraction; -, contraction).

Structure	LEED analysis	Total energy calculation
$\Delta z_1/d_b$	$1.72 \pm 2.2\%$	-1.30%
$\Delta z_2/d_b$	$0.00 \pm 1.6\%$	2.58%
$(d_{12} - d_b)/d_b$	$-0.35 \pm 1.9\%$	-12.5%
$(d_{23} - d_b)/d_b$	$-8.33 \pm 4.9\%$	-2.67%

TABLE III. Total energies (eV) per atom of $\text{Mn}_{100}/\text{Ag}(001)$, $\text{Mn}_{50}\text{Ag}_{50}/\text{Mn}_{50}\text{Ag}_{50}/\text{Ag}(001)$, and $\text{Ag}_{100}/\text{Mn}_{100}/\text{Ag}(001)$ in paramagnetic (PM), ferromagnetic (FM), and antiferromagnetic (AFM) phases with reference to that of $\text{Mn}_{100}/\text{Ag}(001)$ in the paramagnetic state.

System	Total energy (eV)		
	PM	FM	AFM
$\text{Mn}_{100}/\text{Ag}(001)$	0.0	-1.53	-1.60
$\text{Mn}_{50}\text{Ag}_{50}/\text{Mn}_{50}\text{Ag}_{50}/\text{Ag}(001)$	-0.25	-1.64	-1.75
$\text{Ag}_{100}/\text{Mn}_{100}/\text{Ag}(001)$	-0.72	-1.94	-1.96

ergies of $\text{Mn}_{100}/\text{Ag}(001)$, $2\text{Mn}_{50}\text{Ag}_{50}/\text{Ag}(001)$, and $\text{Ag}_{100}/\text{Mn}_{100}/\text{Ag}(001)$ in their paramagnetic (PM), ferromagnetic (FM), and antiferromagnetic (AFM) phases are presented in Table III. For all growth modes, the AFM state is the most stable magnetic state. The formation energy of the bilayer alloy, $E[\text{Mn}_{100}/\text{Ag}(001)] - E[2\text{Mn}_{50}\text{Ag}_{50}/\text{Ag}(001)]$, namely, 150 meV per atom, is much larger than that of a single-layer alloy,

$$\frac{1}{2}\{E[\text{Ag}(001)] + E[\text{Mn}_{100}/\text{Ag}(001)]\} - E[\text{Mn}_{50}\text{Ag}_{50}/\text{Ag}(001)],$$

namely, 8 meV per atom. This result indicates that the bilayer alloy system is more stable than a single-layer surface alloy. Another notable fact in Table III is that $\text{Ag}_{100}/\text{Mn}_{100}/\text{Ag}(001)$ is more stable by 210 meV than $2\text{Mn}_{50}\text{Ag}_{50}/\text{Ag}(001)$. This implies that Mn in the surface layer in $2\text{Mn}_{50}\text{Ag}_{50}/\text{Ag}(001)$ can diffuse into the $\text{Ag}(001)$ substrate, if activated, for example, by annealing. This prediction is in line with our observation that the $c(2 \times 2)$ LEED pattern disappears even after a gentle annealing of 5 min at 400 K. The interlayer spacings were also calculated on $2\text{Mn}_{50}\text{Ag}_{50}/\text{Ag}(001)$ and the results are listed in Table II. Compared with the results of a dynamic LEED analysis, some discrepancies are found in the interlayer spacing.

Considering the results of the LEED analysis and the total energy calculations together, the origin of the $c(2 \times 2)$ structure in $\text{Mn}/\text{Ag}(001)$ at room temperature is definitely the formation of an ordered surface alloy in the first two layers. But this structure is metastable, and there can exist another domain which is more stable energetically such as $\text{Ag}_{100}/\text{Mn}_{100}/\text{Ag}(001)$, as predicted by the total energy calculations. If there exist two different microdomains near the surface, i.e., the bilayer ordered surface alloy [$2\text{Mn}_{50}\text{Ag}_{50}/\text{Ag}(001)$] and the Mn subsurface layer [$\text{Ag}_{100}/\text{Mn}_{100}/\text{Ag}(001)$], then the resulting I - V curve should be calculated by a weighted average of two LEED I - V curves from these two domains according to the ratio of their domain areas. We therefore further refined our fitting of the LEED I - V curves including the ratio of the two domain areas as an additional fitting parameter. Then, an R_p factor that is lower by 0.024 than that of the pure bilayer surface alloy model could be obtained, when the domains are composed of the bilayer surface alloy by 85% and subsurface Mn layer by

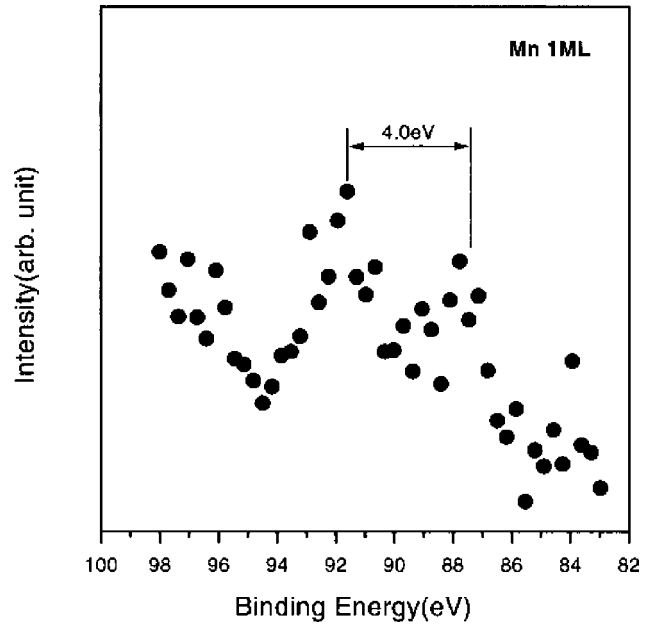


FIG. 3. $3s$ core level spectra of Mn on $\text{Ag}(001)$ at one monolayer thickness.

15%. This means that the bilayer ordered surface alloy structure is a diffusion-limited, thermodynamically metastable system.

The Mn $3s$ XPS core level spectra of nominal 1 ML Mn thickness is presented in Fig. 3. The quality of the data is not good enough to try a detailed curve fitting, but two peaks with an energy splitting of 4.0 eV are clearly observed. This splitting is similar to that observed in bulk Mn.¹⁴ If we interpret this splitting as due to the exchange interaction between the $3s$ core hole and the $3d$ valence electron, this result implies that the local magnetic moment of Mn in this surface alloy state is quite large. Hence, the magnetic energy contribution is thought to be a significant factor in the energetics of ordered alloy formation, as shown in previous experiments and theoretical calculations.^{2,8} Wuttig *et al.*⁸ found with a LEED I - V analysis that Mn deposited on $\text{Cu}(001)$ forms a very stable $c(2 \times 2)$ surface alloy, and also attributed its stability to the magnetic energy contribution due to an enhanced local magnetic moment of surface Mn atoms. This scenario was later confirmed by the observation of Mn in its high-spin state by x-ray absorption spectroscopy.^{15,16}

One may suppose that the formation of a bilayer ordered $\text{Mn}/\text{Ag}(001)$ alloy can be described by an energetic scheme and atomic diffusion process similar to that for the $\text{Mn}/\text{Cu}(001)$ system,¹⁷ but the difference of atomic size and surface free energy is expected to bring about definite differences between the two systems. First, Ag is larger than Cu, and so Mn incorporation into the substrate will happen more easily on $\text{Ag}(001)$ than on $\text{Cu}(001)$.¹⁸ The negligible corrugation of the $\text{Ag}(001)$ $c(2 \times 2)$ Mn surface alloy system compared with that of $\text{Cu}(001)$ $c(2 \times 2)$ Mn can be regarded as a result of this difference of atomic size between Ag and Cu. Second, the surface free energy difference of Ag and Cu is another important factor which makes for the different characteristics of the two systems. It is well known that the surface free energy of Ag (1.302 J m^{-2}) is significantly lower than that of Cu (1.934 J m^{-2}).¹⁹ Hence the atomic exchange

process between Mn and Ag will happen more easily than between Mn and Cu, and so many Ag atoms ejected from the substrate can exist at the surface. Since these Ag adatoms are very mobile, they could form a MnAg alloy structure on the surface by incorporation of Mn subsequently deposited on the surface. A similar behavior of Ag atoms was reported in a previous scanning tunneling microscopy study for Rh/Ag(001).²⁰

The lower surface free energy of Ag than that of Cu also explains the thermodynamic instability of the Mn/Ag(001) system. To stabilize this surface alloy structure through the cancellation of a surface energy difference by a magnetic energy contribution as in the Mn/Cu(001) system, the magnetic moment of Mn in this system has to be larger. The value of the magnetic moment predicted by our *ab initio* calculation is $3.96\mu_B$ for the first layer Mn and $3.55\mu_B$ for the second layer Mn at zero temperature, whereas the experimental magnetic moment of Mn in the surface alloy at room temperature, estimated from the well-known linear relationship between the $3s$ exchange splitting and the local magnetic moment of Mn, is around $2.7\mu_B$.²¹ The discrepancy between the calculated and experimental values appears to come from temperature effects, since a previous neutron scattering experiment²² in a dilute Mn-Ni alloy reported that the Mn magnetic moments at 4.2 K, $3.50\mu_B$, is reduced at room temperature to $2.63\mu_B$. Further, the behavior of a

MnCu alloy was found to be similar to that of the MnNi alloy.²³ These magnetic moments predicted for Mn in the bilayer alloy are similar to that recently calculated, $3.75\mu_B$, for the Mn/Cu(001) system.²⁴ This implies that magnetic effects in the bilayer alloy formation would just be comparable with that in the Mn/Cu(001) system. Hence, the magnetic energy due to the local magnetic moment of Mn might be effective in the formation of an ordered alloy, but insufficient to overcome the large surface energy difference between Mn and Ag. This would explain the relative instability of bilayer Mn ordered alloy on Ag(001) compared to the Mn ordered alloy on Cu(001), as evidenced by the swift disappearance of the bilayer alloy ordered structure on Ag(001) even for the gentle annealing at 400 K.

In conclusion, we showed that the $c(2\times 2)$ LEED pattern of Mn/Ag(001) is due to bilayer ordered surface alloy formation and the local magnetic moment of Mn atom is instrumental in the formation of this surface alloy. This type of surface alloy formation by the effects of magnetism deserves more detailed studies with various tools, as another important example of the complexity of thin films.

We thank A. J. Freeman for his careful reading of this paper and S. Blügel and Y. Gauthier for helpful information. This work was supported in part by the Basic Future Technology Project and the BSRI program (97-2440), Ministry of Science and Technology in Korea, and by the ONR (Grant No. N00014-94-1-0030) at Northwestern University.

¹M. Wuttig *et al.*, Surf. Sci. **331-333**, 659 (1995).

²S. Blügel, Appl. Phys. A: Solids Surf. **63**, 595 (1996).

³D. A. Newstead *et al.*, J. Phys. C **21**, 3777 (1988).

⁴B. T. Jonker *et al.*, Phys. Rev. B **39**, 1399 (1989).

⁵W. F. Egelhoff *et al.*, J. Vac. Sci. Technol. A **8**, 1582 (1990).

⁶J. E. Ortega and F. J. Himpsel, Phys. Rev. B **47**, 16 441 (1993).

⁷P. Schieffer *et al.*, Surf. Sci. **352-354**, 823 (1996).

⁸M. Wuttig, Y. Gauthier, and S. Blügel, Phys. Rev. Lett. **70**, 3619 (1993).

⁹S. H. Kim *et al.*, Phys. Rev. B **55**, 7904 (1997).

¹⁰P. J. Rous, Prog. Surf. Sci. **39**, 3 (1992); A. Wander *et al.*, Phys. Rev. Lett. **67**, 626 (1991).

¹¹V. L. Moruzzi, J. F. Janak, and A. R. Williams, *Calculations of Electronic Properties of Metals* (Pergamon, New York, 1978).

¹²J. B. Pendry, J. Phys. C **13**, 937 (1980).

¹³E. Wimmer *et al.*, Phys. Rev. B **24**, 864 (1981).

¹⁴F. R. McFeely *et al.*, Solid State Commun. **15**, 1051 (1974).

¹⁵W. O'Brien and B. P. Tonner, J. Appl. Phys. **76**, 6468 (1994).

¹⁶W. O'Brien *et al.*, J. Phys.: Condens. Matter **5**, L515 (1993).

¹⁷M. Wuttig, T. Flores, and S. Junghans, Surf. Sci. **371**, 1 (1997); **371**, 14 (1997).

¹⁸F. F. Abraham, Phys. Rev. Lett. **46**, 546 (1981); B. Legrand *et al.*, Phys. Rev. B **41**, 4422 (1990).

¹⁹L. Mezey and J. Giver, Jpn. J. Appl. Phys., Part 1 **21**, 1569 (1987).

²⁰S.-L. Chang *et al.*, Phys. Rev. B **53**, 13 747 (1996).

²¹F. J. Himpsel, J. Magn. Mater. **102**, 261 (1992).

²²J. W. Cable and H. R. Child, Phys. Rev. B **10**, 4607 (1974).

²³J. R. Davis and T. J. Hicks, J. Phys. F **9**, 753 (1979).

²⁴O. Rader *et al.*, Phys. Rev. B **55**, 5404 (1997).